

# Alternating quarantine for sustainable mitigation of COVID-19

Dror Meidan<sup>1</sup>, Nava Schulmann<sup>2,3</sup>, Reuven Cohen<sup>1</sup>, Simcha Haber<sup>1</sup>, Eyal Yaniv<sup>4</sup>, Ronit Sarid<sup>5</sup> & Baruch Barzel<sup>1,6,\*</sup>

1. Department of Mathematics, Bar-Ilan University, Ramat-Gan, Israel
2. Department of Mechanical Engineering, Politecnico di Milano, Milan, Italy
3. MIMESIS, Inria, Strasbourg, France
4. Graduate School of Business Administration, Bar Ilan University, Ramat-Gan, Israel
5. Faculty of Life Sciences & Institute of Nanotechnology and Advanced Materials, Bar Ilan University, Ramat-Gan, Israel
6. Gonda Multidisciplinary Brain Research Center, Bar-Ilan University, Ramat-Gan, Israel

\* Correspondence: [baruchbarzel@gmail.com](mailto:baruchbarzel@gmail.com)

Lacking a drug or vaccine, the current strategy to contain the COVID-19 pandemic is by means of social distancing, specifically mobility restrictions and lock-downs. Such measures impose a hurtful toll on the economy, and are difficult to sustain for extended periods. The challenge is that selective isolation of the symptomatic patients is insufficient to control SARS-CoV-2, due to its relatively long incubation period, in which individuals experience no symptoms, but may already contribute to the spread. How then do we isolate these *invisible* pre-symptomatic spreaders? Here we propose an alternating quarantine strategy, in which at every instance, half of the population remains under lock-down while the other half continues to be active, maintaining a routine of weekly succession between activity and quarantine. Under this regime, if an individual was exposed during their active week, by the time they complete their quarantine they will, in most cases, begin to exhibit symptoms. Hence this strategy isolates the majority of pre-symptomatic individuals during their infectious phase, leading to a rapid decline in the viral spread - all while sustaining a continuously active economy at 50% capacity.

Battling the spread of SARS-CoV-2, most countries have resorted to social distancing policies, imposing restrictions [1], from complete lock-downs, to severe mobility constraints [2–5], gravely impacting socioeconomic stability and growth. Most current projections on COVID-19 indicate that such policies must be put in place for extended periods (typically months) to avoid reemergence of the epidemic once lifted [6, 7]. This, however, may be unsustainable, as individual social and economic needs will, at some point surpass the perceived risk of the pandemic.

The challenge is that while we isolate the symptomatic patients, exposed individuals become infectious a few days prior to the onset of symptoms [8–13] (Fig. 1a). During this pre-symptomatic stage, they behave as *invisible spreaders*, who continue to interact with their network, unaware of their potential infectiousness. To address this we propose an *alternating quarantine* (AQ) strategy, based on two principals: (i) Complete isolation of all symptomatic individuals, as already practiced at present [1]; (ii) Partitioning of the remaining population into two cohorts that undergo weekly successions of quarantine and routine activity. Other periodic cycles, *e.g.*, bi-weekly, or 5 working

days vs. 9 quarantine days, may also be considered. The partition must be at household level, guaranteeing all cohabitants are in the same cohort. Hence while Cohort 1 remains active, Cohort 2 stays at home and vice versa, ensuring little interaction between the cohorts (Fig. 1d). This provides a highly efficient mitigation, alongside continuous socio-economic productivity, in which half of the workforce remains active at each point in time.

The AQ strategy limits social mixing [14], while providing an outlet for people to sustain their economic and social routines. At the same time it treats one of the main obstacles for COVID-19 mitigation - the prevalence of invisible spreaders. To illustrate this consider an individual in Cohort 1 who was active during week 1, and therefore might have been infected. This individual will soon enter their pre-symptomatic stage, precisely the stage in which they are *invisible*, and hence contribute most to the spread. However, according to the AQ routine, they will be confined to their homes during week 2, and consequently, they will be isolated precisely during their suspected pre-symptomatic period. If, by the end of week 2 they continue to show no symptoms, most chances are that they are, in fact, healthy, and can, therefore, resume activity in week 3 according to the planned routine. Conversely, if they do develop symptoms during their quarantine, they must remain in isolation, similar to all symptomatic individuals. *Hence, the weekly succession is in resonance with the natural SARS-CoV-2 disease cycle [15], and in practice, leads to isolation of the majority of invisible spreaders. If implemented fully, it guarantees, in each bi-weekly cycle, to prune out the infectious individuals and sustain an active workforce comprising a predominantly uninfected population.*

## Potential challenges

We identify four potential obstacles in AQ that we address below:

**Variability.** While the SARS-CoV-2 disease cycle is well-mapped, as appears in Fig. 1a, there is a significant level of variability across the population. Specifically, the pre-symptomatic stage may, at times, last longer than the average 5 days, with reported instances of up to two weeks [10–13, 16–19]. Such late onset of symptoms may lead to pre-symptomatic spreaders that were not screened during their quarantine week, resulting in a potential *leakage* of infectious individuals into the active cohort. Therefore, in our modeling of the disease, we incorporated such variability in individual transition times between states, congruent with empirically observed levels of individual heterogeneity (Fig. 1c)

**Asymptomatic patients.** An estimated 30% of infected individuals do not experience noticeable symptoms but may still shed the virus and be infectious [20–27]. Such asymptomatic spreaders are overlooked by our AQ strategy, potentially resuming activity in the end of their quarantine shift. Fortunately, lacking symptoms, such as coughing, which promotes virus shedding and dissemination, these asymptomatic individuals are likely less infectious than their symptomatic peers. Furthermore, asymptomatic individuals could very well have lower viral load in their respiratory tract and saliva [28–31]. Therefore, their impact on the SARS-CoV-2 transmission is likely reduced. Despite that, to err on the side of safety, *in our modeling of the spread we use a uniform infection rate, for all individuals - symptomatic or asymptomatic - testing AQ under potentially challenging assumptions.*

**Conformity.** AQ is especially effective under full social cooperation [32], however, similar to any mitigation strategy, such perfect social compliance is difficult to achieve. We, therefore, included

a fraction  $f$  of social defectors, to examine the impact of non cooperative individuals on the effectiveness of AQ. We also outline an implementation plan to increase abidance, discussing specific challenges and merits of the AQ strategy (Fig. 4).

**In-house transmission.** Similar to any quarantine-based strategy, AQ does not limit infection between cohabitants. To reduce such in-house transmission, an independent policy of extended testing and individual isolation must be employed [33]. This track, orthogonal to AQ, is a relevant complement to any proposed quarantine policy. Indeed, AQ is offered to ease the impact of social distancing, not to replace other relevant actions that can exist alongside it.

## Analysis

**Modeling the spread of SARS-CoV-2.** In Fig. 1a we present the SARS-CoV-2 characteristic infection cycle. Upon exposure ( $E$ ) individuals enter a pre-symptomatic period, which lasts, on average  $\sim 5$  days, after which they begin to exhibit mild ( $I_M$ ), severe ( $I_S$ ) or critical ( $I_C$ ) symptoms, leading to hospitalization ( $H$ ), and in acute cases also to ventilation ( $V$ ). Approximately 2 days prior to the onset of symptoms the exposed individuals become infectious, hence, on average, the infectious phase begins 3 days after initial exposure [8]. Spreading the virus continues until the onset of symptoms, at which point the infected individuals enter isolation and cease to contribute to the spread. A fraction of the exposed individuals remain asymptomatic ( $AS$ ), and hence do not isolate, throughout their entire infectious period, beginning on average 4 days posterior to exposure [18]. Hence, the symptomatic carriers spread the disease within an average window of  $\sim 2$  days (purple), while the asymptomatic carriers continue to infect others until their immune response clears the virus.

These time-scales represent the *average* infection cycle, which, in reality, may exhibit variability across the population. This is especially relevant regarding the time for the appearance of symptoms, which, if delayed beyond 1 – 2 weeks, may lead to an infectious crossover between successive terms of activity, *e.g.*, if a person is infected in week 1, and then, lacking symptoms, resumes activity in week 3 (see Fig. 1d). Therefore, for each of the relevant time-scales, *e.g.*, the time from exposure to infectiousness, or the time to develop symptoms, we consider not just the *average*, but the *complete distribution* across the population (Fig. 1c). For example, the probability density function  $P_1(t')$  captures the fraction of exposed individual who exhibit symptoms within  $t \in (t', t' + dt')$  days from exposure. Similarly,  $P_2(t')$  characterizes the transition times between exposure and asymptomatic infectiousness. The broader are  $P_i(t')$ , the greater is the individual variability in transition times between the different disease states. Here we extract  $P_i(t')$  from a Weibull distribution [13], in congruence with the variability observed in other infections of Corona type viruses (Supplementary Section 2).

Allowing such distributed transition times between disease states requires a unique modeling framework, that goes beyond the standard implementation of SIR or SEIR modeling [34–38]. Indeed, transitions such as  $E \rightarrow I$  are typically simulated via a Poissonian process, in which exposed individuals transform into the infected state at a constant rate [39]. This leads to an exponential decay in the number of exposed individuals  $E(t)$  that begins upon exposure, representing a *memory-less* process, whose probability is independent of the time since becoming exposed. Our implementation, in contrast, incorporates the fact that such transitions are characterized not just by their *average* duration *a la* Poisson, but rather by a specified, empirically relevant distribution. The

mathematical implementation of such distributed transition times is detailed in Supplementary Section 1.

To evaluate the infection rate  $\beta$  we collected data on the evolution of the epidemic in 14 different countries [40], and examined the mortality  $D(t)$  at the early stages of the spread, prior to the implementation of social distancing policies (Fig. 2a-f). We use  $D(t)$  since it represents an objective measure. This is, as opposed to  $I(t)$ , the number of (symptomatic) infected individuals, which may be biased by the volume and nature of each country's diagnostics. We find that  $D(t)$  can be well approximated by an exponential inflation of the form  $D(t) \sim e^{kt}$ , with  $k$  narrowly distributed across different countries around  $k \approx 0.25 \text{ days}^{-1}$ . This allows us to extract each country's intrinsic infection rate  $\beta$ , finding that, on average,  $\beta \approx 1.25$  (Fig. 2m).

Using these coefficients we obtained a projection of the expected evolution of the epidemic (Fig. 2n). We also track the expected fraction of hospitalized ( $H(t)$ ) and ventilated ( $V(t)$ ) individuals, which, we find, exceed, by a significant margin, the average national hospitalization/ventilation [41] capacities (Fig. 2o). The expected mortality is captured by  $D(t \rightarrow \infty)$  reaching, absent any mitigation efforts, a level of  $\sim 4\%$  (grey). Next, we examine the behavior of COVID-19 under AQ, together with other relevant strategies.

## Mitigation

To examine the impact of our proposed strategy we track the evolution of  $I(t) = I_M(t) + I_S(t) + I_C(t)$ . First we allow the disease to proliferate unmitigated (Fig. 3a, orange, UM), then at time  $t = t_0$  (dashed vertical line) we instigate our response. Examining four relevant mitigation strategies, we establish a basis upon which to evaluate AQ's performance.

**Full quarantine - FQ** (Fig. 3a, dark green). This represents the *theoretically ideal* response, in which all infectious interactions are fully inhibited, and hence, mathematically, the infection rate is set to  $\beta = 0$ . Such perfect *air-tight* quarantine is, clearly, unrealistic, however, it is useful in the present context, as it provides a baseline for comparison, indeed, setting the bounds for a *perfect* mitigation. Unsurprisingly, we find that FQ leads to a rapid exponential decline in  $I(t)$ , clearing the population of the virus within a typical time-scale of several weeks [33].

**Alternating quarantine - AQ** (Fig. 3a, blue). We now examine the AQ strategy. At  $t = t_0$  we partition the population into two equal groups, cohorts 1 and 2, and have them alternating successively between quarantine and regular activity, in a bi-weekly cycle. We find, again, that  $I(t)$  decays exponentially, albeit at a slower rate, as compared to the *perfect* FQ. *The crucial point, however, is that this decay is now observed, despite the fact that 50% of the population remains continuously active.* AQ achieves this thanks to its weekly periodicity, which is roughly in phase with the natural  $\sim 5$  day cycle of incubation and pre-symptomatic infection.

Next, we consider two natural alternatives to AQ, both designed to sustain socioeconomic activity at a 50% rate:

**Intermittent quarantines - IQ** (Fig. 3a, turquoise). In this strategy [42] society as a whole enters a periodic cycle of active vs. quarantined phases, namely the entire population transitions in unison between staying at home and going to work. Originally proposed in the format of a 4 : 10 periodicity, *i.e.* 4 days of activity separated by 10 days of quarantine, here we examine its performance under a 7 : 7 cycle, to be congruent with our implementation of AQ. We find that

IQ is significantly less effective than AQ, leading not only to higher peak infection, but also to a substantially longer time to return to normalcy.

**Half quarantine - HQ** (Fig. 3a, red). Another mitigation alternative that allows a 50% active workforce is based on a selective quarantine, in which only 50% of the population partakes in socioeconomic activities, while the remaining half is instructed to stay at home. HQ suppresses the rate of infection by reducing social interactions by a factor of one half. Our simulation results indicate, however, that, similarly to IQ, this reduction is insufficient. Indeed,  $I(t)$  continues to proliferate significantly beyond manageable levels, once again, failing to mitigate the disease.

Taken together, we find that AQ provides the most efficient mitigation, bringing us closest to the ideal performance of FQ, without fully shutting down the economy. To understand the origins of the observed AQ advantage, we first consider its alternatives, IQ and HQ. The common root of both strategies is that they reduce the level of interaction by a factor of one half. IQ achieves this by decreasing the interaction *duration*; HQ accomplishes this by diluting the interacting *population*. In this sense, the strength of AQ is that it benefits from both factors (Fig. 5): partitioning the population into cohorts ensures that only half are active at all times - similar to HQ. Yet, the weekly alternations ensure that each cohort remains active only half the time - similar to IQ. *The result is an effective force multiplier, allowing the same amount of net activity - 50% - but with a dramatically enforced mitigation effect.*

**Social conformity** (Fig. 3b - g). In Fig. 3a, we have examined all mitigation strategies under perfect conditions, in which all citizens fully comply with the imposed social restrictions. In reality, however, a certain level of violation is inevitable. Therefore, we now introduce a fraction  $f$  of defectors, who continue their activity at all times, both during their active shift as well as when they are instructed to quarantine. Despite these defection levels, we continue to assume that symptomatic patients remain cooperative. Indeed, not only are COVID-19 symptoms difficult to conceal, but also most individuals, even defectors, do not have the audacity to commit explicit violations, knowingly interacting when they are infectious. We find that AQ continues to suppress the disease, even as defection levels approach  $f = 10\%$  (Fig. 3b - d).

While the majority of infected individuals exhibit mild or no symptoms, a certain percentage may experience severe complications, leading to hospitalization or ventilation, and in some cases to mortality (Fig. 1a). Our mitigation strategy focuses on these undesired paths within the infection track - namely, we aim to decrease mortality  $D(t)$ , and ensure that at their peak,  $H(t)$  and  $V(t)$  do not exceed the national hospitalization and ventilation capabilities. To test this we measured the residual mortality

$$\Delta D = D_S(t \rightarrow \infty) - D_{FQ}(t \rightarrow \infty) \quad (1)$$

where  $D_S(t \rightarrow \infty)$  is the long term mortality under strategy S, *e.g.*, IQ or AQ, and  $D_{FQ}(t \rightarrow \infty)$  is the expected mortality under FQ. Indeed,  $D_{FQ}(t \rightarrow \infty)$  represents inevitable deaths, rooted in infections that occurred prior to our response, and hence  $\Delta D$  captures the *additional* mortality, that our mitigation failed to prevent. In Fig. 3e we measured  $\Delta D$  vs. the defection level  $f$  under IQ (turquoise) and AQ (blue). We find, quite expectantly, that as defection levels rise, so does the residual mortality. However, most crucially, AQ consistently saves more lives, compared to IQ.

To examine the impact of AQ on the severe and critical patients, we measure

$$H_{\text{Peak}} = \max_{t=t_0}^{\infty} H(t), \quad (2)$$

capturing the peak hospital occupancy *after* instigating our response (Fig. 3f). While IQ (turquoise circles) fails to bring  $H_{\text{Peak}}$  within capacity (dashed grey line), AQ (blue circles) sustains a leveled occupancy even under as much as  $f = 20\%$  defection. Hence, AQ is highly robust against partial compliance - a crucial requisite for any practical mitigation strategy. Similar results are also obtained for  $V_{\text{Peak}} = \max_{t=t_0}^{\infty} V(t)$  (Fig. 3g).

## Synergistic measures

Our analysis, up to this point, assumed a *worst case scenario*, in which, aside from our mitigation strategy (AQ, IQ or HQ), all other disease parameters remain unchanged. In reality, however, in addition to AQ, or any other strategy for that matter, we can expect, at the least, that standard prophylactic behaviors will continue to be practiced. Indeed, personal hygiene, face-masks and contact avoidance can reduce infections significantly, without taking any toll on the economy. Therefore, in practice, the infection rate  $\beta = 1.25$ , inferred from the early, pre-mitigation stages of the epidemic, will likely be reduced as we gradually relax social distancing and resume normalcy. We, therefore, examine the performance of the different mitigation strategies also under a reduced  $\beta$ , capturing the synergistic effect offered by prophylactic practices. In the *intermediate case* we set  $\beta = 1$ , a 20% reduction in the rate of infection (Fig. 3h - n), and as our *best case scenario*, we examined  $\beta = 0.75$ , capturing a 40% drop in infectiousness (Fig. 3o - u). Under these more favorable conditions, AQ's performance approaches even closer to the ideal FQ (*e.g.*, Fig. 3o), and, strikingly, it exhibits robust mitigation, even under 20 or 30% defection (Fig. 3k,r).

More generally, our AQ strategy can, and should, be reinforced by other complementary policies, to ensure mitigation success. For example, the selective protection of vulnerable populations, avoidance of social gatherings and the establishment of isolation facilities to reduce in-house transmission. All of these policies can be instigated alongside, rather than instead, of AQ. One may also consider alternative periodic cycles. For instance, a 5 : 9 cycle, in which the active shifts last only 5 days. In this version of AQ, society enters a routine in which each cohort is allowed a 5 day work-week, then observes population-wide quarantine over the weekend. Such adaptations will further improve the performance of AQ beyond its already established effectiveness.

## Implementation

The AQ strategy works best when the two cohorts are fully separated, lacking all forms of cross-group infection. The partition should, therefore, be implemented at a household level, ensuring all cohabitants are in the same activity/quarantine cycle. A simple way to achieve this is to base the partition on a person's living address. This provides an additional benefit, in the case of apartment buildings, as neighbors, who risk cross-infection through shared building facilities, are included in the same cohort. Each individual/household will be informed by their local authority of their quarantine schedule, and in parallel, employers will be instructed to resume their activity in shifts, with only half the workforce at a time. Businesses will be held legally liable and incur significant fines in case of violation.

Instances of conflict between a person’s assigned shift and their employer’s specific requirements will be resolved on a *case by case* basis - all while strictly adhering to the household-based partition. The resulting cohorts will likely deviate from an exact balanced cut, due to differences in household sizes and other constraints, however, the crucial point is, that the partition need not be perfect, as, indeed, the cohorts must be decoupled, but not necessarily equal in size. Therefore, some level of flexibility is enabled to accommodate specific constraints or special needs.

While AQ is found to be efficient even under partial social abidance ( $f$ ), there are several recommended measures to increase the level of cooperation:

**Communication.** To engage the population towards cooperation, the first step is to communicate the rationale behind AQ, its potential effectiveness, and the individual compliance required for its rapid success. This appeals to people’s intrinsic motivation [43], a crucial component of conformity, but often also insufficient due to the *tragedy of the commons*. We therefore map the *drivers*, that enhance people’s desire to cooperate, vs. the *inhibitors*, that stand in their way [44, 45], and set appropriate *moderators* to enforce the drivers and suppress the inhibitors (Fig. 4).

**Inhibitors** (Fig. 4a). During its lock-down cycle, the quarantined cohort is required to stay at home for one week, indeed, a challenge, however, being limited in time, it is significantly less stressful than an extended several week quarantine. We identify four motivators to violate the quarantine: *Business* - going to work, *Schooling* - arrangements for child care, *Services and supplies* - visiting public market places or service centers, and *Outdoors* - exercise or strolling with children or pets. Of these, the latter, being in the open, is least risky, and also practically unavoidable, as young children and pets require routine outdoor activity. We, therefore, focus on moderators especially for the first three inhibitors.

**Moderators** (Fig. 4c). While moderation can be achieved via coercion, *e.g.*, law enforcement, it is most effectively implemented by creating supporting frameworks for cooperation. For example, in the AQ framework, defection for business and schools is simply not possible. Indeed, since businesses are legally required to divide their workforce into shifts, one cannot go to work out of cycle. Similarly, schools will not admit children who are not in the presently active cohort. Therefore, the main challenge is to deter violators from visiting public places for supplies or services. This can be achieved by (i) instructing the population to prepare in advance for a full week of isolation; (ii) establishing a logistic and psychological support network to aid citizens who encounter unexpected needs; (iii) creating a dedicated app to issue exit permits only to members of the active cohort. The app in (iii) will not violate citizen privacy in any way, but only indicate if the device holder is in Cohort 1 or 2. Residents will be asked to present their app to enter shopping centers or public institutions.

Together, the proposed moderators create a framework that not only diminishes incentives for defection, *e.g.*, by logistically supporting the isolated cohort, but also eliminates the means, as, indeed, aside from daily outdoor strolling, practically all other out of home activities are automatically barred by the AQ framework itself. The strength of this implementation plan is that it achieves this without coercion, namely that almost no enforcement via authorized forces against individuals is required, maintaining a level of trust between citizen and government and securing personal freedoms. To complete the plan, at the end of the isolation week, all isolated residents will be required to report their health status via the app. Those who report symptoms, as well as their cohabitants, will remain at their *stay-home* status, going into isolation until their verified

recovery.

## Alternating vs. population-wide quarantine

The proven advantages of AQ indicate that it is not merely an *exit strategy* from a period of population-wide quarantine (PWQ), but may actually serve as an initial response strategy, *instead* of such quarantine. To understand this we consider both the implementation challenges as well as the epidemiological merits of both strategies.

Intuitively, one would expect a time-limited PWQ to be more effective than AQ, both in terms of mitigation - isolating larger parts of the population, as well as in terms of implementation - not having to resolve between the two cohorts. Our analysis, however, indicates that AQ has crucial advantages on both fronts. The implementation challenge of PWQ is that it requires people to stay at home for a period of several weeks, in order for the mitigation to take effect. For example, in Fig. 3a we found that a 100% perfectly implemented quarantine (FQ), which is, indeed, a theoretical construction only, still required 5 – 7 weeks to achieve a significant gain over the disease. Under these conditions, one cannot implement a truly complete lock-down. Essential services, supply chains and some parts of the market must remain active, since households cannot retain supplies and remain self-sufficient for such extended periods. Therefore, a practical PWQ can at most be implemented at a level of 70 – 80% [46].

In contrast, the AQ scheme requires citizens to isolate only for a single week at a time. Hence, the quarantined cohort can truly enter, for just one week, a complete lock-down regime, in which they avoid purchasing supplies or any other services. Consequently, under AQ, while a larger part of the population is active at all times, the quarantined cohort, can sustain a much stricter lock-down routine. As a result not only is the economy more productive, with 50% of the population continuously active, but the mitigation outcome is also comparable, and under some conditions even superior. To demonstrate this, in Fig. 6 we examine the impact of PWQ, imposed at a level of 50, 60, 70, 75 and 80% (red to yellow). We then compare it with the performance of AQ (blue). Note that the 80% PWQ case represents the practical upper bound for any realistic PWQ.

We find that AQ’s mitigation effect (blue) falls in between that of a 75 (orange) to 80% (yellow) PWQ. Yet whereas PWQ at such levels severely compromises the economy and imposes significant social and psychological stress, AQ accomplishes a similar effect, while sustaining a productive economy, and allowing a manageable routine for the individual. Therefore, we believe AQ to be the optimal strategy to manage our socioeconomic activity alongside COVID-19 mitigation.

## Discussion

The efficiency of the AQ strategy is rooted in three principals: (i) Partitioning the population into two cohorts reduces the volume of infectious interactions, comparable to a 50% quarantine (HQ). (ii) Working in weekly succession reduces the total duration of interaction within each cohort, similar to intermittent quarantines (IQ). Combined these two factors together, allows a similar net volume of socioeconomic activity as in any of the above strategies, HQ or IQ, *but with a multiplied mitigation effect*. While (i) and (ii) are independent of the succession period, *e.g.*, daily or weekly, our design of AQ around *weekly* alternations provides a third advantage: (iii) It synchronizes the quarantine phase with the suspected incubation period of each cohort, hence systematically pruning

out the invisible SARS-CoV-2 spreaders.

Alternating quarantine can be implemented as an *exit strategy*, following a period of suppression via population-wide quarantine. As such, it allows a gradual reigniting of a dormant economy, while minimizing the risk of a recurring outbreak. However, our results indicate that it can also serve as a primary mitigation strategy, with comparable impact to that of a strict population-wide quarantine (Fig. 6).

A crucial strength of AQ is its robustness against defection, under some conditions withstanding as much as 30% violators. Nevertheless, we believe that the weekly relief, allowing people an outlet to continue their activity for half of the time, may, itself, increase cooperation levels. Indeed, while a complete lock-down is extremely stressful for the individual, the AQ bi-weekly routine relaxes the burden, and may encourage compliance. Moreover, with workplaces and schools forced to operate in fully partitioned shifts, and with our suggested mobile app and logistic support network, the implementation of AQ has little dependence neither on self-motivation nor on externally enforced cooperation (Fig. 4). Indeed, schools and employment will naturally drive the population between activity and inactivity, with *enforcement* only required to treat outdoor recreation - which, in any case, has little contribution to the infection. This affords us a degree of freedom to allow certain levels of *authorized* defection, *i.e.* a quota of essential workers, relieved from the quarantine cycles.

Our analysis assumes an incubation period that is of the order of a single week, specifically in our simulations, we set it at an average of 5 days. The rationale however is more general, and can be adapted to longer or shorter incubation times, simply by tuning the periodicity of the alternating shifts, keeping them congruent with the natural cycle of the infection.

More broadly, we consider the fact that there is, inherently, some level of uncertainty regarding the disease parameters. We therefore examined the worst case scenario, in which the infection rate during the active weeks is the same as that of the unmitigated spread. In practice, however, we expect many additional measures to be implemented in parallel to the quarantines, such as extended testing for infections, face-masks and strict hygienic regulations at the workplace. At the least, we expect standard prophylactic behavior, such as avoiding contact or banning social gatherings, to be observed also during each cohort's active week. Such norms, that will continue until COVID-19 is fully eradicated, will further push down  $\beta$ , enhancing the effectiveness of our strategy even beyond the reported results.

Here, we have mainly discussed the epidemiological merits of AQ, and its implementation, in broad strokes, as a national strategy. In practice, different societies, as well as different economic sectors, will require specific adaptations. For example, while AQ is naturally compatible with non-professional industries, in which workers can be arbitrarily partitioned into shifts, it becomes more challenging in professional workplaces, where key personnel may be irreplaceable. Specific solutions, therefore, must be tailored to accommodate different economies and sectors. In light of the unambiguous mitigating advantage, we believe such adaptations are, by far, worth the effort.

**Data availability.** All codes to reproduce, examine and improve our proposed analysis are available at <https://github.com/drormeidán/ALDCOVID19>.

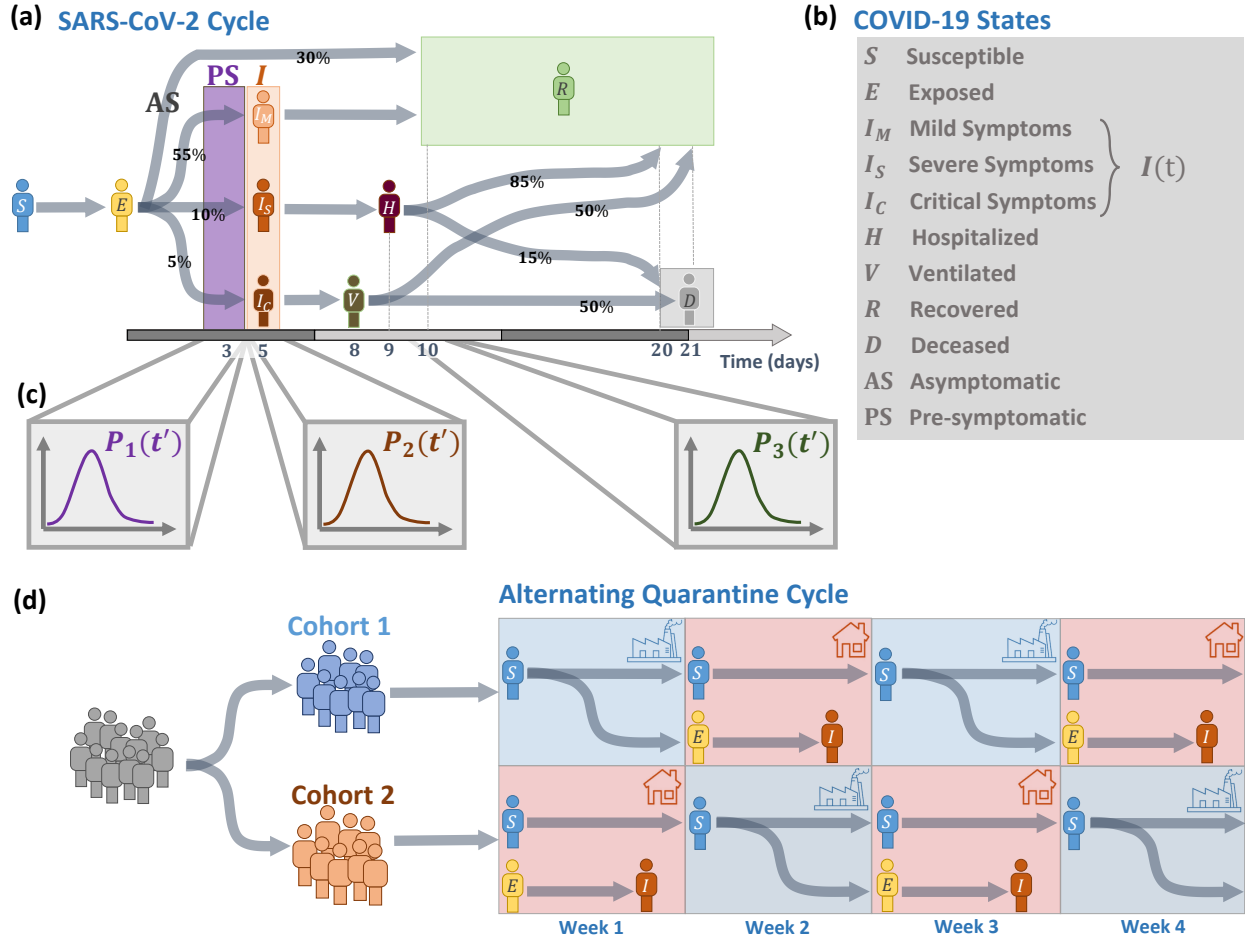


**FIG. 1: The cycles of SARS-CoV-2 and COVID-19 vs. those of the Alternating quarantine strategy.** (a) We collected data on the transitions between the SARS-CoV-2 and COVID-19 states and constructed the characteristic disease cycle. Upon exposure ( $E$ ) individuals enter an average 5 day incubation period prior to developing symptoms - mild ( $I_M$  at a rate of 55%), severe ( $I_S$ , 10%) or critical ( $I_C$ , 5%). The remaining 30% are asymptomatic ( $AS$ ). Infectiousness begins typically 3 days after exposure for symptomatic carriers, and 4 days for the asymptomatic ( $AS$ ). The *infection window* (violet) captures the invisible pre-symptomatic ( $PS$ ) spreading phase, in which individuals are infectious, but lack symptoms. Upon the onset of symptoms, infected individuals are isolated and cease to infect others. Consequently, asymptomatic individuals have a longer infection window, which extends until their transition to  $R$ . As the disease progresses a fraction of the infected population may require hospitalization ( $H$ ) or ventilation ( $V$ ), leading, with some probability to mortality ( $D$ ). (b) The compartments of the COVID-19 cycle. We denote by  $I(t)$  the unity of all *symptomatic* individuals ( $I = I_M + I_S + I_C$ ). This corresponds to the diagnosed case count in each country (Fig. 2), which covers mainly the patients who exhibit symptoms. (c) While the illustrated cycle in (a) captures the average transition times between all states, in reality, some level of variability exists across the population. This is captured by the distribution  $P_i(t')$ . For example the individual transition time from  $E$  to  $PS$ , whose average is 3 days, is extracted from  $P_1(t')$  (purple). (d) Alternating quarantine (AQ) splits the population into separate cohorts that alternate between periods of activity (going to work, blue) and inactivity (staying at home, red). Following their active week (week 1) individuals in Cohort 1 may become exposed (yellow), in which case they will sit out their suspected pre-symptomatic period at home (week 2). By the end of their quarantine week they will likely develop symptoms (orange) and remain in isolation until their full recovery. Those who did not develop symptoms during their week of quarantine are most likely uninfected (blue) and can resume activity in their upcoming active shift (week 3). Therefore the AQ cycle behaves as a *ratchet*, consistently quarantining the invisible spreaders, and hence, removing, with each weekly succession, infectious individuals from the active population.

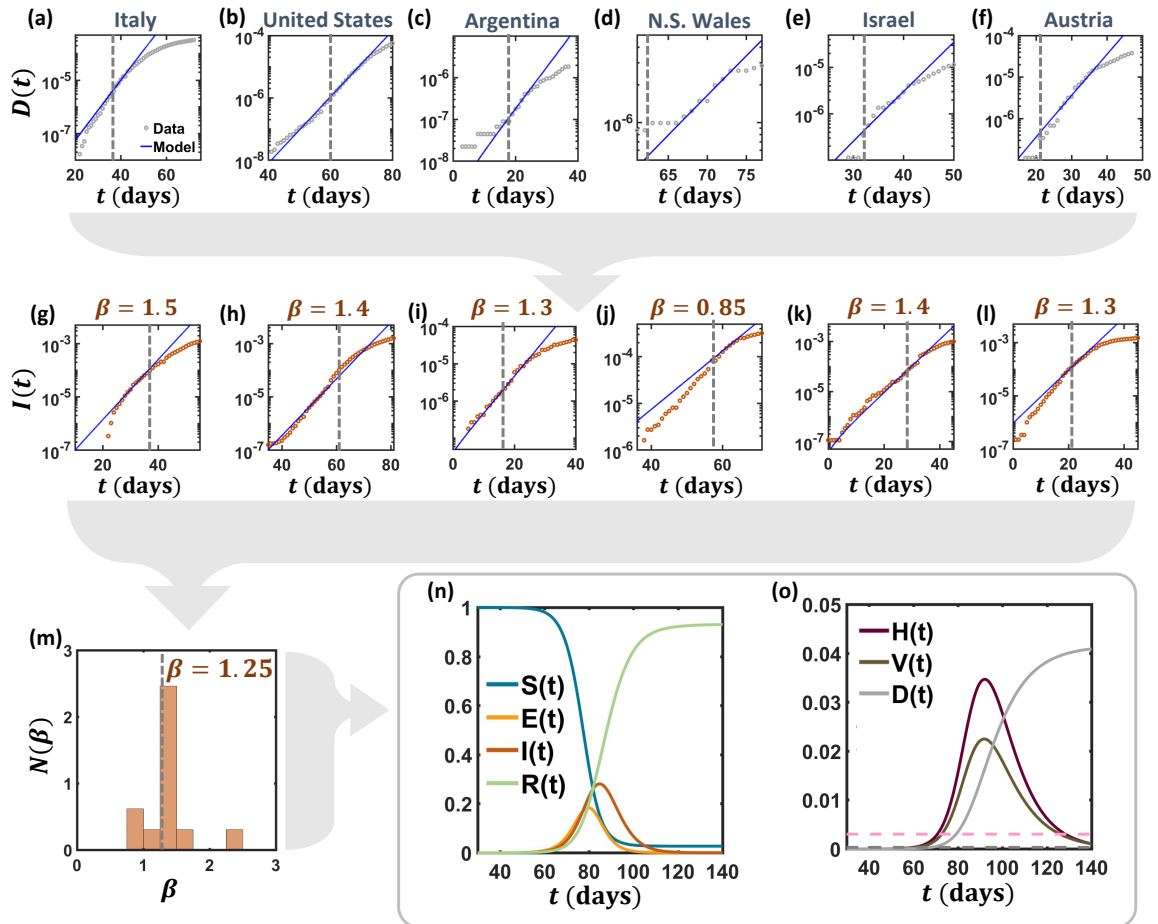


FIG. 2: **Extracting SARS-CoV-2 infection rate.** (a) - (f) We collected data [40] on the mortality  $D(t)$  vs.  $t$  (grey circles) as observed in 14 different countries (only six are shown here), and measured its exponential growth rate (black solid lines). This allowed us to evaluate the observed infection rate  $\beta$  in every country. In each panel we also indicate the time for the institution of social distancing policies (dashed lines). Exponential growth typically continues for a period of 1 to 2 weeks posterior to such policies. We, therefore, used only the data up to one week after the implementation of social distancing to evaluate the exponential growth. (g) - (l) To further examine our data-extracted  $\beta$ , we used it to predict  $I(t)$  in each country, based on all reported cases. We find that the data (orange circles) is well-approximated by our projections (black solid lines), further confirming the relevance of our modeling framework, and its extracted parameters. Since asymptomatic individuals are, in the majority of cases not diagnosed, we evaluate infection levels via  $I(t) = I_M(t) + I_S(t) + I_C(t)$ , as defined in Fig. 1b. (m) Histogram of inferred  $\beta$  values across the 14 countries. Infection rates are distributed around an average of  $\beta = 1.25$ . Hence, in our simulations we take this value to represent the rate of infection, in the absence of all prophylactic measures. In reality, standard behavioral practices, such as personal hygiene or avoidance of physical contact, may push  $\beta$  to significantly lower values. Hence, in our simulations we incorporate three scenarios: worst case -  $\beta = 1.25$ , intermediate case -  $\beta = 1$  and best case -  $\beta = 0.75$ , all of which, we believe represent rather conservative estimates of the actual  $\beta$ . (n) Taking  $\beta = 1.25$  we simulated the projected evolution of the COVID-19 pandemic, without any preventive measures. (o) We focus on three crucial parameters that characterize the severity of the projected spread: mortality  $D(t)$  (grey), hospitalization level  $H(t)$  (purple) and the number of individuals requiring ventilation  $V(t)$  (brown). Absent any intervention, at their peak, both  $H(t)$  and  $V(t)$  exceed, by a large margin, the average national hospitalization/ventilation capacities, estimated at  $3 \times 10^{-3}$  (dashed pink line) and  $7 \times 10^{-4}$  (dashed grey line), respectively [41].

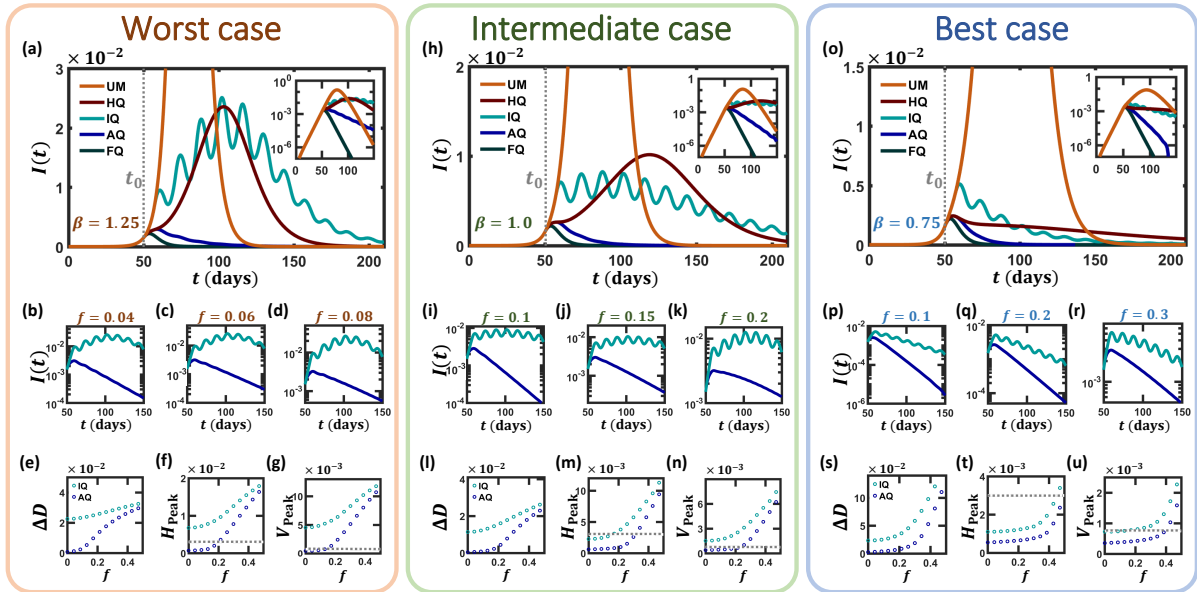


FIG. 3: **The impact of Alternating quarantine.** (a) The infection  $I(t)$  vs.  $t$  of the unmitigated epidemic (UM, orange), as obtained under the worst case scenario of  $\beta = 1.25$ . At  $t_0 = 50$  days (dashed grey line) we instigate four competing mitigation strategies: Full quarantine (FQ, dark green), Alternating quarantine (AQ, blue), Intermittent quarantines (IQ, turquoise) and Half quarantine (HQ, red). We find that, under these conditions, apart from the *idealized* FQ, only AQ provides successful mitigation (log-scale appears in the inset). (b) - (d) To examine the robustness of AQ (blue) and IQ (turquoise) against partial compliance, we allowed a fraction  $f$  of quarantine violators. AQ continues to performs well even under  $f = 0.08$  (d), capturing an 8% defection level. (e) Residual mortality  $\Delta D$  (1) vs. the defection rate  $f$ . (f) Peak hospitalization  $H_{\text{Peak}}$  vs.  $f$ . AQ (blue) ensures that occupancy is within the average national hospitalization capacity (dashed grey line) even when challenged by an  $f = 0.2$  defection rate. IQ (turquoise), on the other hand, overburdens the health case system, beyond its maximal capacity already at  $f = 0$ . (h) - (n) A similar analysis, this time assuming that for  $t > t_0$ , the infection rate drops by 20% to  $\beta = 1$ . AQ retains its mitigation advantage, now being able to sustain even higher defection rates. (o) - (u) In our best case scenario we take the infection rate, posterior to our intervention ( $t > t_0$ ) to be  $\beta = 0.75$ .

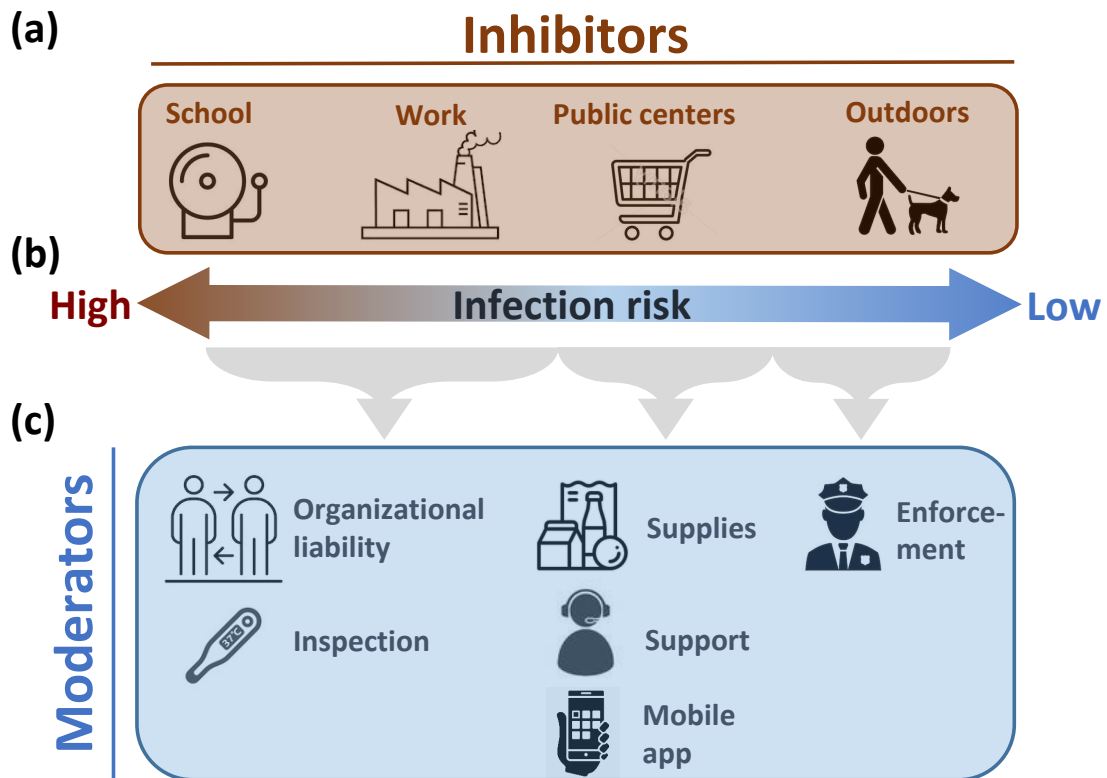


FIG. 4: **Driving social conformity for Alternating quarantine.** (a) We identify four needs that inhibit potential cooperation: child care arrangements, work, purchasing supplies or services and outdoor activities. (b) Infection risk is highest under extensive and continuous interactions, such as in school or at work, and least significant during open-air activities, such as strolling or exercising. We therefore focus on moderators mainly for the first three inhibitors. (c) To enhance social compliance we seek moderator that encourage conformity in lieu of coercive enforcement: *School and work*. Due to their liability, schools and workplaces will be naturally prohibited for the quarantined cohort, as both will be required to abide by the AQ routine, and therefore will not admit workers or students of the inactive cohort. In addition, routine inspections for symptoms will expose potential defectors who wish to conceal their infection. *Public centers*. We consider three moderators to deter individuals from seeking services or supplies: (i) instruct the population to obtain sufficient supplied in advance for a single week; (ii) establish a support network in case of unexpected needs; (iii) create a mobile app confirming an individual's cohort (1 or 2), that must be displayed upon entry to public centers. Outdoor activity could be moderated by enforcement, however, since it poses little infection risk, we believe such activity should, in practice, be ignored.

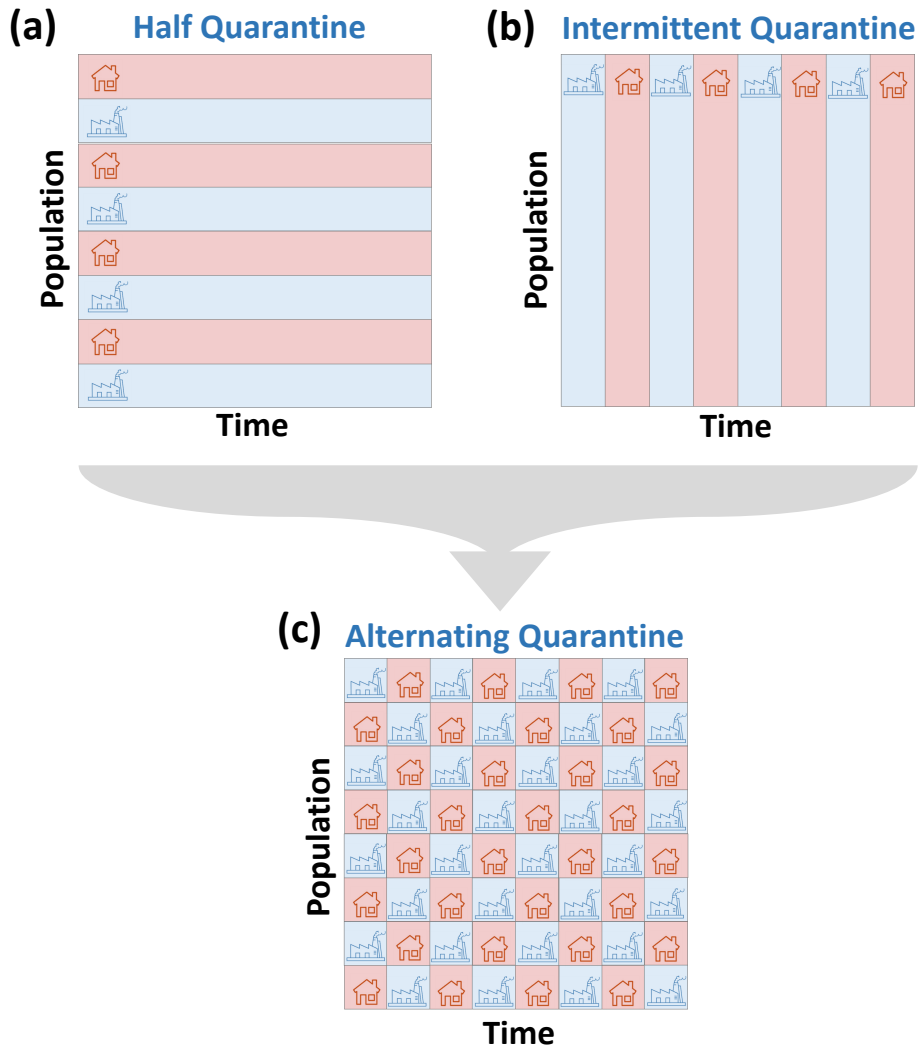


FIG. 5: **The multiplicative effect of Alternating quarantine.** We consider three strategies - all allowing socioeconomic activity (blue) vs. quarantine (red) at half capacity. (a) The Half quarantine strategy reduces infection by diluting the active *population*, hence decreasing the rate of infectious interactions. (b) Intermittent quarantines achieve a similar outcome by diminishing the duration of activity, hence reducing the *time* of infectious interactions. (c) Alternating quarantines combine both effects: on the one hand interactions are limited to individuals within each cohort - diluting the population. On the other hand these cohorts experience intermittent cycles of work/home - diminishing interaction duration.

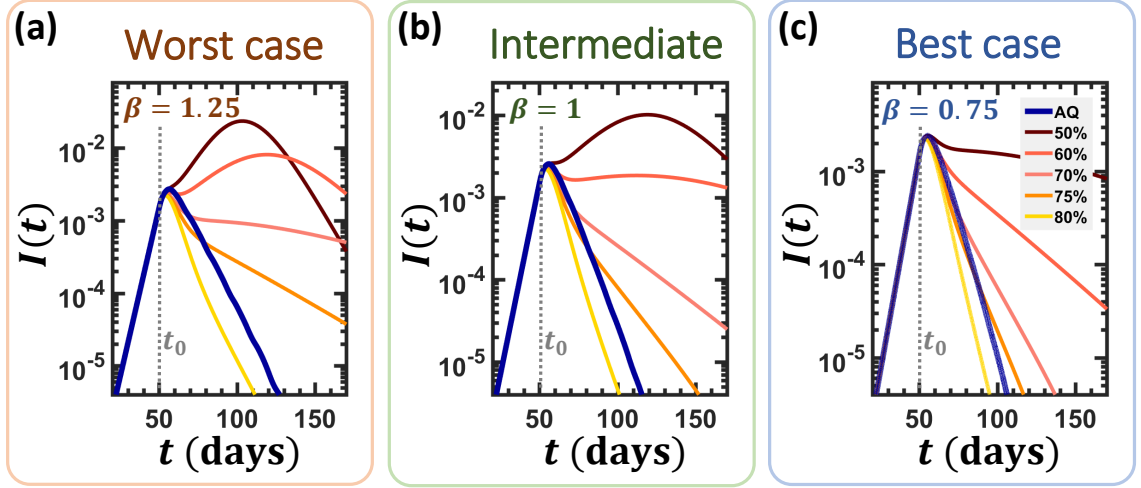


FIG. 6: **Alternating quarantine vs. population-wide quarantine.** (a) Infection level  $I(t)$  vs.  $t$  as obtained for  $\beta = 1.25$ . At  $t_0 = 50$  days (dashed grey lines) we initiate our mitigation via Alternating quarantine (AQ, blue). We also examined population-wide quarantines at 50, 60, 70, 75 and 80% levels (red to yellow). Despite having half of the population active at all times, AQ's mitigation is comparable to that of an 80% population-wide quarantine. Hence, instead of an extremely hurtful socioeconomic shutdown of 75 to 80%, indeed the practical upper bound of social distancing policies, AQ offers a similar outcome under a significantly reduced socioeconomic price-tag. (b) - (c) Similar results are observed also under our intermediate ( $\beta = 1$ ) and best case ( $\beta = 0.75$ ) scenarios.

- 
- [1] R.M. Anderson, H. Heesterbeek, S. Klinkenberg and T.D. Hollingsworth. How will country-based mitigation measures influence the course of the COVID-19 epidemic? *The Lancet*, 395:10228, 2020.
- [2] Moritz U. G. Kraemer, Chia-Hung Yang, Bernardo Gutierrez, Chieh-Hsi Wu, Brennan Klein, David M. Pigott, , Louis du Plessis, Nuno R. Faria, Ruoran Li, William P. Hanage, John S. Brownstein, Maylis Layan, Alessandro Vespignani, Huaiyu Tian, Christopher Dye, Oliver G. Pybus, and Samuel V. Scarpino. The effect of human mobility and control measures on the covid-19 epidemic in china. *Science*, 2020.
- [3] Alex Arenas, Wesley Cota, Jesus Gomez-Gardenes, Sergio Gomez, Clara Granell, Joan T. Matamalas, David Soriano-Panos, and Benjamin Steinegger. Derivation of the effective reproduction number  $r$  for covid-19 in relation to mobility restrictions and confinement. *medRxiv*, 2020.
- [4] Benjamin Maier and Dirk Brockmann. Effective containment explains subexponential growth in recent confirmed covid-19 cases in china. *Science*, page eabb4557, 04 2020.
- [5] Bnaya Gross, Zhiguo Zheng, Shiyun Liu, Xiaoqi Chen, Alon Sela, Jianxin Li, Daqing Li, and Shlomo Havlin. Spatio-temporal propagation of covid-19 pandemics. *medRxiv*, 2020.
- [6] J. Hellewell *et al.* Feasibility of controlling COVID-19 outbreaks by isolation of cases and contacts. *Lancet Global Health*, 8:488, 2020.
- [7] Anatoly Zhigljavsky, Roger Whitaker, Ivan Fesenko, Yakov Kremnitzer, and Jack Noonan. Comparison of different exit scenarios from the lock-down for covid-19 epidemic in the uk and assessing uncertainty of the predictions. *medRxiv*, 2020.
- [8] Q. Li *et al.* Early transmission dynamics in Wuhan, China, of novel coronavirus-infected pneumonia. *N Engl J. Med.*, 382:1199, 2020.
- [9] WHO. Coronavirus disease (COVID-2019) situation report 30. 2020.
- [10] Luca Ferretti, Chris Wymant, Michelle Kendall, Lele Zhao, Anel Nurtay, Lucie Abeler-Dörner, Michael Parker, David Bonsall, and Christophe Fraser. Quantifying sars-cov-2 transmission suggests epidemic control with digital contact tracing. *Science*, 2020.
- [11] NM Ferguson, D Laydon, G Nedjati-Gilani, N Imai, K Ainslie, M Baguelin, S Bhatia, A Boonyasiri, Z Cucunubá, G Cuomo-Dannenburg, et al. Impact of non-pharmaceutical interventions (npis) to reduce covid-19 mortality and healthcare demand. imperial college covid-19 response team, 2020.
- [12] Jantien A Backer, Don Klinkenberg, and Jacco Wallinga. Incubation period of 2019 novel coronavirus (2019-ncov) infections among travellers from wuhan, china, 20–28 january 2020. *Eurosurveillance*, 25, 2020.
- [13] Natalie M Linton, Tetsuro Kobayashi, Yichi Yang, Katsuma Hayashi, Andrei R Akhmetzhanov, Sungmok Jung, Baoyin Yuan, Ryo Kinoshita, and Hiroshi Nishiura. Incubation period and other epidemiological characteristics of 2019 novel coronavirus infections with right truncation: a statistical analysis of publicly available case data. *Journal of clinical medicine*, 9, 2020.
- [14] Per Block, Marion Hoffman, Isabel J. Raabe, Jennifer Beam Dowd, Charles Rahal, Ridhi Kashyap, and Melinda C. Mills. Social network-based distancing strategies to flatten the covid 19 curve in a post-lockdown world, 2020.
- [15] Guy P. Nason. Rapidly evaluating lockdown strategies using spectral analysis: the cycles behind new daily covid-19 cases and what happens after lockdown, 2020.
- [16] Qun Li, Xuhua Guan, Peng Wu, Xiaoye Wang, Lei Zhou, Yeqing Tong, Ruiqi Ren, Kathy SM Leung, Eric HY Lau, Jessica Y Wong, et al. Early transmission dynamics in wuhan, china, of novel coronavirus-infected pneumonia. *New England Journal of Medicine*, 2020.
- [17] Xuan Jiang, Simon Rayner, and Min-Hua Luo. Does sars-cov-2 has a longer incubation period than sars and mers? *Journal of medical virology*, 2020.
- [18] Yinon M Bar-On, Avi Flamholz, Rob Phillips, and Ron Milo. Sars-cov-2 (covid-19) by the numbers. *eLife*, 9, 2020.

- [19] Stephen A Lauer, Kyra H Grantz, Qifang Bi, Forrest K Jones, Qulu Zheng, Hannah R Meredith, Andrew S Azman, Nicholas G Reich, and Justin Lessler. The incubation period of coronavirus disease 2019 (covid-19) from publicly reported confirmed cases: estimation and application. *Annals of internal medicine*, 2020.
- [20] Yang Tao, Panke Cheng, Wen Chen, Peng Wan, Yaokai Chen, Guodan Yuan, Junjie Chen, Da Huo, Ge Guan, Dayu Sun, et al. High incidence of asymptomatic sars-cov-2 infection, chongqing, china. 2020.
- [21] Kenji Mizumoto, Katsushi Kagaya, Alexander Zarebski, and Gerardo Chowell. Estimating the asymptomatic proportion of coronavirus disease 2019 (covid-19) cases on board the diamond princess cruise ship, yokohama, japan, 2020. *Eurosurveillance*, 25, 2020.
- [22] Xingfei Pan, Dexiong Chen, Yong Xia, Xinwei Wu, Tangsheng Li, Xueting Ou, Liyang Zhou, and Jing Liu. Asymptomatic cases in a family cluster with sars-cov-2 infection. *The Lancet Infectious Diseases*, 20, 2020.
- [23] Xiaoxia Lu, Liqiong Zhang, Hui Du, Jingjing Zhang, Yuan Y Li, Jingyu Qu, Wenxin Zhang, Youjie Wang, Shuangshuang Bao, Ying Li, et al. Sars-cov-2 infection in children. *New England Journal of Medicine*, 2020.
- [24] Jaffar A Al-Tawfiq. Asymptomatic coronavirus infection: Mers-cov and sars-cov-2 (covid-19). *Travel medicine and infectious disease*, 2020.
- [25] Philippe Colson et al. Children account for a small proportion of diagnoses of sars-cov-2 5 infection and do not exhibit greater viral loads than adults.
- [26] Huan Song, Jun Xiao, Jiajun Qiu, Jin Yin, Huazhen Yang, Rui Shi, and Wei Zhang. A considerable proportion of individuals with asymptomatic sars-cov-2 infection in tibetan population. *medRxiv*, 2020.
- [27] Yuanyuan Dong, Xi Mo, Yabin Hu, Xin Qi, Fan Jiang, Zhongyi Jiang, and Shilu Tong. Epidemiology of covid-19 among children in china. *Pediatrics*, 2020.
- [28] Yang Liu, Li-Meng Yan, Lagen Wan, Tian-Xin Xiang, Aiping Le, Jia-Ming Liu, Malik Peiris, Leo LM Poon, and Wei Zhang. Viral dynamics in mild and severe cases of covid-19. *The Lancet Infectious Diseases*, 2020.
- [29] Yi Xu, Xufang Li, Bing Zhu, Huiying Liang, Chunxiao Fang, Yu Gong, Qiaozhi Guo, Xin Sun, Danyang Zhao, Jun Shen, et al. Characteristics of pediatric sars-cov-2 infection and potential evidence for persistent fecal viral shedding. *Nature Medicine*, 2020.
- [30] Xi He, Eric HY Lau, Peng Wu, Xilong Deng, Jian Wang, Xinxin Hao, Yiu Chung Lau, Jessica Y Wong, Yajuan Guan, Xinghua Tan, et al. Temporal dynamics in viral shedding and transmissibility of covid-19. *medRxiv*, 2020.
- [31] Kelvin Kai-Wang To, Owen Tak-Yin Tsang, Wai-Shing Leung, Anthony Raymond Tam, Tak-Chiu Wu, David Christopher Lung, Cyril Chik-Yan Yip, Jian-Piao Cai, Jacky Man-Chun Chan, Thomas Shiu-Hong Chik, et al. Temporal profiles of viral load in posterior oropharyngeal saliva samples and serum antibody responses during infection by sars-cov-2: an observational cohort study. *The Lancet Infectious Diseases*, 2020.
- [32] Alex Tawse, Vanessa M Patrick, and Dusya Vera. Crossing the chasm: Leadership nudges to help transition from strategy formulation to strategy implementation. *Business Horizons*, 62, 2019.
- [33] Shen Chen Yaneer Bar-Yam. COVID-19: How to win, 2020.
- [34] L. Hufnagel, D. Brockmann and T. Geisel. Forecast and control of epidemics in a globalized world. *Proc. Natl. Acad. Sci. USA*, 101:15124–9, 2004.
- [35] P.S. Dodds, R. Muhamad and D.J. Watts. An experimental study of search in global social networks. *Science*, 301:827–829, 2003.
- [36] A. Vespignani. Modelling dynamical processes in complex socio-technical systems. *Nature Physics*, 8:32–39, 2012.
- [37] D. Brockmann, V. David and A.M. Gallardo. Human mobility and spatial disease dynamics. *Reviews of Nonlinear Dynamics and Complexity*, 2:1, 2009.
- [38] R. Pastor-Satorras, C. Castellano, P. Van Mieghem and A. Vespignani. Epidemic processes in complex

- networks. *Rev. Mod. Phys.*, 87:925–958, 2015.
- [39] B. Barzel and O. Biham. Binomial moment equations for stochastic reaction systems. *Phys. Rev. Lett.*, 106:150602–5, 2011.
- [40] E. Dong, H. Du and L. Gardner. An interactive web-based dashboard to track COVID-19 in real time. *The Lancet Infectious Diseases*, 2020.
- [41] <https://data.worldbank.org/indicator/sh.med.beds.zs>.
- [42] Omer Karin, Yinon M. Bar-On, Tomer Milo, Itay Katzir, Avi Mayo, Yael Korem, Boaz Dudovich, Eran Yashiv, Amos J. Zehavi, Nadav Davidovich, Ron Milo, and Uri Alon. Adaptive cyclic exit strategies from lockdown to suppress covid-19 and allow economic activity. *medRxiv*, 2020.
- [43] Michael R Baumann and Bryan L Bonner. An Expectancy Theory Approach to Group Coordination: Expertise, Task Features, and Member Behavior. *Journal of Behavioral Decision Making*, 30, 2017.
- [44] V H Vroom. *Work and Motivation*. Wiley, New York NY, 1964.
- [45] Ata ul Musawir, Saipol Bari Abd-Karim, and Mohd Suhaimi Mohd-Danuri. Project governance and its role in enabling organizational strategy implementation: A systematic literature review. *International Journal of Project Management*, 38, 2020.
- [46] Harshad Khadilkar, Tanuja Ganu, and Deva P Seetharam. Optimising lockdown policies for epidemic control using reinforcement learning, 2020.

# **SUPPLEMENTARY**

# **INFORMATION**

# Alternating quarantine for sustainable mitigation of COVID-19

## Supplementary Information

### I. MODELLING THE COVID-19 EPIDEMIC SPREAD

#### A. Modeling the unmitigated epidemic

We consider a population of  $N$  individuals, of which  $\mathbb{S}(t)$  are susceptible,  $\mathbb{E}(t)$  are exposed,  $\mathbb{I}(t)$  are infected,  $\mathbb{R}(t)$  are recovered,  $\mathbb{D}(t)$  are deceased,  $\mathbb{H}(t)$  are hospitalized and  $\mathbb{V}(t)$  are ventilated. Hence,  $\mathbb{S}(t) + \mathbb{E}(t) + \mathbb{I}(t) + \mathbb{R}(t) + \mathbb{V}(t) + \mathbb{H}(t) + \mathbb{D}(t) = N$  for all  $t$ . The exposed population consists of individuals who have been exposed to the virus, but are not yet infectious. This population is divided into two sub-populations,  $\mathbb{E}_S(t)$  and  $\mathbb{E}_{NS}(t)$ , where  $\mathbb{E}_S(t)$  are the exposed individuals that will develop symptoms eventually, whereas  $\mathbb{E}_{NS}(t)$  are the exposed individuals who will recover without ever developing symptoms, i.e. asymptomatic.

The infected population  $\mathbb{I}$  is also subdivided into several sub-populations,  $\mathbb{I}_{NS}(t)$  are the non-symptomatic individuals, who never develop symptoms,  $\mathbb{I}_{PS}(t)$  are the pre-symptomatic individuals, who are currently non-symptomatic, but will eventually develop symptoms. Of the symptomatic,  $\mathbb{I}_M(t)$ ,  $\mathbb{I}_S(t)$ , and  $\mathbb{I}_C(t)$  represent mild, severe and critical condition infected individuals, respectively. The hospitalized population is denoted by  $\mathbb{H}$ , and the ventilated by  $\mathbb{V}$ . Note that hospitalized individuals are a sub-group of the infected, and that ventilated individuals are a sub-group of the hospitalized. However, in our modeling we treat these populations as distinct, hence  $\mathbb{I}$ ,  $\mathbb{H}$  and  $\mathbb{V}$  represent different compartments with no overlap.  $\mathbb{R}$  are the recovered individuals, who are assumed not to be susceptible to the infection again, at least not during the current outbreak, and  $\mathbb{D}$  are the deceased individuals, who did not survive the disease. The transition cycle appears if Fig. 7.

In order to model the transitions between the states, we write the rate equations for the different population sizes. For some of the transitions, there is an empirical estimate on the distribution of the transition time between the states. Thus, in order to make the model realistic, we use the empirical distribution rather than a Markov process. In order to simplify the equations, we use the notation

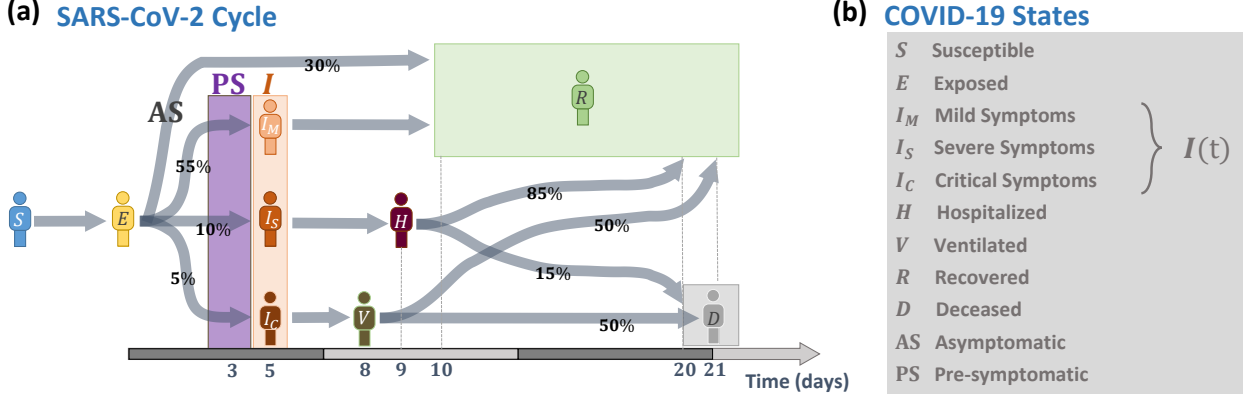


FIG. 7: The infection cycle of SARS-CoV-2.

$$\frac{d\mathbb{E}_+(t)}{dt} = \beta(\mathbb{I}_{NS}(t) + \mathbb{I}_{PS}(t)) \frac{\mathbb{S}(t)}{N}, \quad (3)$$

to capture the positive contribution to the exposed population, due to interaction with  $\mathbb{I}$  individuals around the time  $t$ . As symptomatic individuals are isolated, this contribution is proportional to the number of infected individuals with no symptoms,  $\mathbb{I}_{NS}(t) + \mathbb{I}_{PS}(t)$ , and to the probability  $\mathbb{S}/N$  for them to interact with a susceptible individual. The rate of infection is  $\beta$ . Of all individuals infected around  $t - t'$ , a fraction  $P(t')$  will transition to the  $I$  state at time  $t$ , and therefore the rate of reduction in  $\mathbb{E}$  (or contribution to  $\mathbb{I}$ ) at time  $t$  is captured by the convolution

$$P * \frac{d\mathbb{E}_+}{dt} = \int_0^t P(t') \frac{d\mathbb{E}_+(t-t')}{dt} dt'. \quad (4)$$

Equation (4) sums over all individuals exposed from  $t = 0$  until the present time  $t$ , who will transition from  $\mathbb{E}$  to  $\mathbb{I}$  around the time  $t$ . Below we use the notation of Eqs. (3) and (4) also for different states within  $\mathbb{E}$  ( $\mathbb{E}_S, \mathbb{E}_{NS}$ ) and for different transitions ( $P_i(t')$ ).

To write the equations, we consider the normalized populations  $S(t) = \mathbb{S}(t)/N, I(t) = \mathbb{I}(t)/N, E(t) = \mathbb{E}(t)/N$ , etc., capturing the fraction of individuals in each state. We arrive at the following equations, incorporating all transitions

$$\frac{dS}{dt} = -\beta S(t)(I_{NS}(t) + I_{PS}(t)) \quad (5)$$

$$\frac{dE_{NS}}{dt} = \beta S(t)(I_{NS}(t) + I_{PS}(t)) - P_1 * \frac{dE_{NS+}}{dt} \quad (6)$$

$$\frac{dE_S}{dt} = (1 - P_{NS})\beta S(t)(I_{NS}(t) + I_{PS}(t)) - P_1 * \frac{dE_{S+}}{dt} \quad (7)$$

$$\frac{dI_{NS}}{dt} = P_1 * \frac{dE_{NS+}}{dt} - P_2 * \frac{dE_{NS+}}{dt} \quad (8)$$

$$\frac{dI_{PS}}{dt} = P_3 * \frac{dE_{S+}}{dt} - P_4 * \frac{dE_{S+}}{dt} \quad (9)$$

$$\frac{dI_M}{dt} = P_M P_4 * \frac{dE_{S+}}{dt} - r_{MR} I_M \quad (10)$$

$$\frac{dI_S}{dt} = P_S P_4 * \frac{dE_{S+}}{dt} - r_{SH} I_S \quad (11)$$

$$\frac{dI_C}{dt} = P_C P_4 * \frac{dE_{S+}}{dt} - r_{CV} I_C \quad (12)$$

$$\frac{dH}{dt} = r_{SH} I_S - P_{HR} r_{HR} H - P_{HD} r_{HD} H \quad (13)$$

$$\frac{dV}{dt} = r_{CV} I_C - P_{VR} r_{VR} V - P_{VD} r_{VD} V \quad (14)$$

$$\frac{dR}{dt} = P_2 * \frac{dE_{NS+}}{dt} + P_{HR} r_{HR} H + P_{VR} r_{VR} V + r_{MR} I_M \quad (15)$$

$$\frac{dD}{dt} = P_{HD} r_{HD} H + P_{VD} r_{VD} V \quad (16)$$

Here  $P_i(t')$  represent the density functions for the transition times between the different states:  $i = 1$ , transition time from  $E_{NS}$  to  $I_{NS}$ ;  $i = 2$ , transition from  $E_{NS}$  to  $R$ ;  $i = 3$ , transition from  $E_S$  to  $I_{PS}$ ;  $i = 4$ , transition from  $E_S$  to  $I_M, I_S$  or  $I_C$ , namely from exposure to appearance of symptoms. We focus on these four distributions both because there exists empirical data by which to construct them, but also because they represent the most relevant transitions for the crucial stages in the disease cycle. the parameters  $P_M, P_S$ , and  $P_C$  represent the probabilities to become mild (0.55), severe (0.1) or critical (0.05);  $P_{AB}$  is the probability to transition from state  $A$  to  $B$  (where  $A$  and  $B$  are states) and  $r_{AB}$  are the rates of transitions.  $P_{NS}$  is the probability to become infected but non-symptomatic (0.3), see Fig. 7.

## B. Modeling alternating quarantine

To track the dynamics of COVID-19 under alternating quarantine we first partition the population into 2 groups that alternate between the lock-down state L and the free state F. In each of these groups there is a fraction  $f$  of defectors D and  $1 - f$  of cooperators C. This divides all individuals into four distinct classes: LC, LD, FC and FD, capturing the cooperators/defectors in the locked-down/free groups. Since the defectors are active every week, we do not distinguish between the LD and FD groups, and simply denote them by D. We use superscript to denote an individual's class, hence, *e.g.*,  $E^{LC}(t)$  represents the amount of exposed individuals who are in the lock-down group and are cooperative. These individuals will not contribute to the infection, as they comply with the stay-home instructions. Conversely,  $E^D(t)$  captures the defecting individuals, who choose to remain active and violate the lock-down. Together with  $E^{FC}(t)$ , the exposed individuals in the F group, they will contribute to spreading the virus.

Infections are caused by all exposed individuals who remain active, whether officially or by defection. As explained above, the infected are always isolated, even if defective, hence all  $I$  individuals, aside from  $I_{PS}$  and  $I_{NS}$ , are excluded from the process of infection. This results in two sets of equations. For the free group we write

$$\frac{dS^{FC}}{dt} = -\beta S(t) \left( I_{NS}^{FC}(t) + I_{PS}^{FC}(t) + I_{NS}^D(t) + I_{PS}^D(t) \right) \quad (17)$$

$$\frac{dE_{NS}^{FC}}{dt} = \beta S(t) \left( I_{NS}^{FC}(t) + I_{PS}^{FC}(t) + I_{NS}^D(t) + I_{PS}^D(t) \right) - P_1 * \frac{dE_{NS+}^{FC}}{dt} \quad (18)$$

$$\frac{dE_S^{FC}}{dt} = (1 - P_{NS})\beta S(t) \left( I_{NS}^{FC}(t) + I_{PS}^{FC}(t) + I_{NS}^D(t) + I_{PS}^D(t) \right) - P_1 * \frac{dE_{S+}^{FC}}{dt} \quad (19)$$

$$\frac{dI_{NS}^{FC}}{dt} = P_1 * \frac{dE_{NS+}^{FC}}{dt} - P_2 * \frac{dE_{NS+}^{FC}}{dt} \quad (20)$$

$$\frac{dI_{PS}^{FC}}{dt} = P_3 * \frac{dE_{S+}^{FC}}{dt} - P_4 * \frac{dE_{S+}^{FC}}{dt} \quad (21)$$

$$\frac{dI_M^{FC}}{dt} = P_M P_4 * \frac{dE_{S+}^{FC}}{dt} - r_{MR} I_M^{FC} \quad (22)$$

$$\frac{dI_S^{FC}}{dt} = P_S P_4 * \frac{dE_{S+}^{FC}}{dt} - r_{SH} I_S^{FC} \quad (23)$$

$$\frac{dI_C^{FC}}{dt} = P_C P_4 * \frac{dE_{S+}^{FC}}{dt} - r_{CV} I_C^{FC} \quad (24)$$

$$\frac{dH^{FC}}{dt} = r_{SH} I_S^{FC} - P_{HR} r_{HR} H^{FC} - P_{HD} r_{HD} H^{FC} \quad (25)$$

$$\frac{dV^{FC}}{dt} = r_{CV} I_C^{FC} - P_{VR} r_{VR} V^{FC} - P_{VD} r_{VD} V^{FC} \quad (26)$$

$$\frac{dR^{FC}}{dt} = P_2 * \frac{dE_{NS+}^{FC}}{dt} + P_{HR} r_{HR} H^{FC} + P_{VR} r_{VR} V^{FC} + r_{MR} I_M^{FC} \quad (27)$$

$$\frac{dD^{FC}}{dt} = P_{HD} r_{HD} H^{FC} + P_{VD} r_{VD} V^{FC} \quad (28)$$

For the quarantined population the equations are

$$\frac{dS^{LC}}{dt} = 0 \quad (29)$$

$$\frac{dE_{NS}^{LC}}{dt} = -P_1 * \frac{dE_{NS+}^{LC}}{dt} \quad (30)$$

$$\frac{dE_S^{LC}}{dt} = -P_1 * \frac{dE_{S+}^{LC}}{dt} \quad (31)$$

$$\frac{dI_{NS}^{LC}}{dt} = P_1 * \frac{dE_{NS+}^{LC}}{dt} - P_2 * \frac{dE_{NS+}^{LC}}{dt} \quad (32)$$

$$\frac{dI_{PS}^{LC}}{dt} = P_3 * \frac{dE_{S+}^{LC}}{dt} - P_4 * \frac{dE_{S+}^{LC}}{dt} \quad (33)$$

$$\frac{dI_M^{LC}}{dt} = P_M P_4 * \frac{dE_{S+}^{LC}}{dt} - r_{MR} I_M^{LC} \quad (34)$$

$$\frac{dI_S^{LC}}{dt} = P_S P_4 * \frac{dE_{S+}^{LC}}{dt} - r_{SH} I_S^{LC} \quad (35)$$

$$\frac{dI_C^{LC}}{dt} = P_C P_4 * \frac{dE_{S+}^{LC}}{dt} - r_{CV} I_C^{LC} \quad (36)$$

$$\frac{dH^{LC}}{dt} = r_{SH} I_S^{LC} - P_{HR} r_{HR} H^{LC} - P_{HD} r_{HD} H^{LC} \quad (37)$$

$$\frac{dV^{LC}}{dt} = r_{CV} I_C^{LC} - P_{VRLC} r_{VR} V - P_{VD} r_{VD} V^{LC} \quad (38)$$

$$\frac{dR^{LC}}{dt} = P_2 * \frac{dE_{NS+}^{LC}}{dt} + P_{HR} r_{HR} H + P_{VR} r_{VR} V + r_{MR} I_M \quad (39)$$

$$\frac{dD^{LC}}{dt} = P_{HD} r_{HD} H^{LC} + P_{VD} r_{VD} V^{LC} \quad (40)$$

Finally, for the defectors we have

$$\frac{dS^D}{dt} = -\beta S(t) \left( I_{NS}^{FC}(t) + I_{PS}^{FC}(t) + I_{NS}^D(t) + I_{PS}^D(t) \right) \quad (41)$$

$$\frac{dE_{NS}^D}{dt} = \beta S(t) \left( I_{NS}^{FC}(t) + I_{PS}^{FC}(t) + I_{NS}^D(t) + I_{PS}^D(t) \right) - P_1 * \frac{dE_{NS+}^D}{dt} \quad (42)$$

$$\frac{dE_S^D}{dt} = (1 - P_{NS}) \beta S(t) \left( I_{NS}^{FC}(t) + I_{PS}^{FC}(t) + I_{NS}^D(t) + I_{PS}^D(t) \right) - P_1 * \frac{dE_{S+}^D}{dt} \quad (43)$$

$$\frac{dI_{NS}^D}{dt} = P_1 * \frac{dE_{NS+}^D}{dt} - P_2 * \frac{dE_{NS+}^D}{dt} \quad (44)$$

$$\frac{dI_{PS}^D}{dt} = P_3 * \frac{dE_{S+}^D}{dt} - P_4 * \frac{dE_{S+}^D}{dt} \quad (45)$$

$$\frac{dI_M^D}{dt} = P_M P_4 * \frac{dE_{S+}^D}{dt} - r_{MR} I_M^D \quad (46)$$

$$\frac{dI_S^D}{dt} = P_S P_4 * \frac{dE_{S+}^D}{dt} - r_{SH} I_S^D \quad (47)$$

$$\frac{dI_C^D}{dt} = P_C P_4 * \frac{dE_{S+}^D}{dt} - r_{CV} I_C^D \quad (48)$$

$$\frac{dH^D}{dt} = r_{SH} I_S^D - P_{HR} r_{HR} H^D - P_{HD} r_{HD} H^D \quad (49)$$

$$\frac{dV^D}{dt} = r_{CV} I_C^D - P_{VR^D} r_{VR} V - P_{VD} r_{VD} V^D \quad (50)$$

$$\frac{dR^D}{dt} = P_2 * \frac{dE_{NS+}^D}{dt} + P_{HR} r_{HR} H + P_{VR} r_{VR} V + r_{MR} I_M \quad (51)$$

$$\frac{dD^D}{dt} = P_{HD}r_{HD}H^D + P_{VD}r_{VD}V^D \quad (52)$$

To set the initial conditions we consider the response time  $t_0$  when we employ our intervention. At this time point the state of the system is given by  $S(t_0), E(t_0), I(t_0), R(t_0)$ . We first partition them into two equal groups, each with a fraction  $f$  of defectors. Hence at the intervention point  $t_0$  we have

$$\begin{aligned} S^{\text{FC}}(t_0) &= S^{\text{LC}}(t_0) = \frac{1}{2}(1-f)S(t_0), & S^{\text{D}}(t_0) &= fS(t_0), \\ E^{\text{FC}}(t_0) &= E^{\text{LC}}(t_0) = \frac{1}{2}(1-f)E(t_0), & E^{\text{D}}(t_0) &= fE(t_0), \\ I^{\text{FC}}(t_0) &= I^{\text{LC}}(t_0) = \frac{1}{2}(1-f)I(t_0), & I^{\text{D}}(t_0) &= fI(t_0), \\ R^{\text{FC}}(t_0) &= R^{\text{LC}}(t_0) = \frac{1}{2}(1-f)R(t_0), & R^{\text{D}}(t_0) &= fR(t_0), \\ H^{\text{FC}}(t_0) &= H^{\text{LC}}(t_0) = \frac{1}{2}(1-f)H(t_0), & H^{\text{D}}(t_0) &= fH(t_0), \\ V^{\text{FC}}(t_0) &= V^{\text{LC}}(t_0) = \frac{1}{2}(1-f)V(t_0), & V^{\text{D}}(t_0) &= fV(t_0), \\ D^{\text{FC}}(t_0) &= D^{\text{LC}}(t_0) = \frac{1}{2}(1-f)D(t_0), & D^{\text{D}}(t_0) &= fD(t_0). \end{aligned} \quad (53)$$

Setting the initial condition according to Eq. (53) we solve Eqs. (17) – (52) for a period of 7 days. We then switch between the L and F groups, setting  $S^{\text{LC}}(t) = S^{\text{FC}}(t), E^{\text{LC}}(t) = E^{\text{FC}}(t) \dots$  and vice versa, proceeding to solve the equations for an additional 7 days. We continue with such weekly iterations, until we reach steady-state where  $I(t \rightarrow \infty) \rightarrow 0$ .

### C. Modeling alternating quarantine with a 5 : 9 cycle

Another possible policy is a scheme with alternating groups, each free for a week and in quarantine for the following week, which also has full quarantine during the weekends. Here, there is no incentive for defection during the weekend, as all businesses and workplaces are closed. This also makes monitoring the quarantine easier, as all the population is at the *stay-home* state, and therefore prohibits weekend defection.

In order to model the epidemic spreading in this population, Eqs. (17) – (52) are used for the different groups during working weekdays, whereas for the weekends, Eqs. (29) – (40) are used for the entire population.

### D. Implementation details

The equations were solved using a Runge-Kutta stepper. the convolution integrals were evaluated numerically using a standard rectangle approximation. Distributions  $P_1$  to  $P_4$  were estimated using the Weibull distribution. See Section II for details.

For the alternating quarantine scheme, Eqs. (17) – (52) were solved numerically, where it should be noted that the convolution integrals are calculated for the *same group*, *i.e.* the convolution for the quarantine group for a time when it was free (say a week earlier) is done on the values for what

was then the free group. In simple words, the convolution terms *remember* the states of the free (quarantines) group from the the time it was quarantined (free).

## II. DATA ANALYSIS AND PARAMETER SELECTION

### A. Constructing the distributions $P_i(t')$

Most of the parameters described in Section I were chosen based on observed values of the characteristic SARS-CoV-2 infection cycle. For the density functions  $P_i(t')$ ,  $i = 1, \dots, 4$ , we used a Weibull distribution, inspired by other infections of the Corona variety. To estimate the parameters of the Weibull distribution we collected data on the average  $T_{\text{Av}}$  and median  $T_{\text{Med}}$  of the relevant transition times [13, 18]. This allows to infer the Weibull parameters  $\lambda$  and  $k$  via

$$\begin{aligned} T_{\text{Av}} &= \lambda \Gamma(1 + 1/k); \\ T_{\text{Med}} &= \lambda (\ln 2)^{1/k}. \end{aligned}$$

See Table I for the different values of mean, and median we have used.

Duration	Mean	Median	$\lambda$	$k$
$P_1(t')$	4	3.44	4.42	1.47
$P_2(t')$	10	8.6	11.04	1.47
$P_3(t')$	2	1.72	2.21	1.47
$P_4(t')$	5	4.3	5.52	1.47

TABLE I: **Estimating the distribution parameters.** With data on the average and mean transition times, we reconstructed the distributions  $P_i(t')$ .

### B. Estimating the rate infection $\beta$

The parameter  $\beta$  incorporates both the rate of interaction between a Susceptible person and an Infectious one (be it asymptomatic or pre-symptomatic), and the probability of infection per interaction. Hence we expect  $\beta$  to depend on different aspects of social behavior, personal hygiene routines and contagion characteristics of the pathogen, whose specific parameters are hidden. As a consequence, we need to infer  $\beta$  from observation. As the last step of model calibration,  $\beta$  depends on the other parameters of the model, *e.g.*, if the mean period of contagion is shortened, *ceteris paribus*,  $\beta$  will increase.

As the disease spreads, precautions like social distancing and wearing masks affect both the rate of interaction and the probability of infection. That is,  $\beta$  changes over time. Being conservative, we have chosen to use a value of  $\beta$  reflecting the period *before* such measures were taken.

We have used daily data for the number of confirmed cases and the number of fatalities in several countries. The data set was compiled by and obtained from the Johns Hopkins University Center

for Systems Science and Engineering (JHU CSSE) on April 11<sup>th</sup> 2020 and is available online here: <https://data.humdata.org/dataset/novel-coronavirus-2019-ncov-cases> [40].

The number of confirmed cases may be biased as a result of limited availability of tests. The number of fatalities, in contrast, is more objective and therefore considered more reliable. Still, in many places deaths out of hospital were not counted, regardless of cause. Moreover,  $D(t)$  and  $\beta$  are separated by a few compartments in the model, causing the calculation to be more involved. To treat this, we first used the number of deceased to estimate  $\beta$ , then tested the *goodness* of fit on the number of confirmed cases  $I(t)$ . As can be seen in Figure 8 (and Fig. 2 of main text), the results are satisfactory with very good agreement, with the one exception of Norway, where our retrieval of  $I(t)$  shows some deviation.

As mentioned above,  $\beta$  changes over time as more countermeasures are taken. We have decided to calibrate the model using data starting 3 days before lock-down, as prior to that cases may have been missed by an unready system and ending 10 days after lock-down, when the lock-down starts affecting the number of fatalities. When fitting for the number of confirmed cases, a shorter period was considered. See Table II for the period of estimation per country.

We have chosen countries having prominent number of cases for which reliable data is available. We have also aimed to get a balanced representation, as much as possible, between southern and northern hemisphere countries.

For every country we estimated  $\beta$  by choosing the value  $\hat{\beta}$  minimizing mean squared error between model prediction and true number of deceased, throughout the period starting 3 days before lock-down and ending 10 days after. See Figure 8 for results per country and Figure 9 for the overall distribution of  $\hat{\beta}$ .

Country	Population	First case	Lock-down	$\hat{\beta}$
Italy	60	10	48	1.5
USA	328	1	61	1.4
Argentina	45.1	42	58	1.3
N. S. Wales	8.1	5	62	0.85
Israel	8.9	32	64	1.4
Austria	8.9	35	55	1.3
Spain	46.9	11	51	2.3
Germany	83	6	62	1.4
Norway	5.4	36	49	0.95
South Korea	51.3	1	None	1
Colombia	50.8	45	64	1.3
Belgium	11.6	14	57	1.4
Hubei, China	58.5	1	2	1.3
England	56	1	46	1.05

TABLE II: **Estimating  $\beta$  per country.** Population is given in millions. First case and Lock-down are given in days relative to 22/1. The parameter  $\hat{\beta}$  represents the estimation for  $\beta$ , as extracted from the relevant country data. See Fig. 9 for a histogram of  $\hat{\beta}$ .

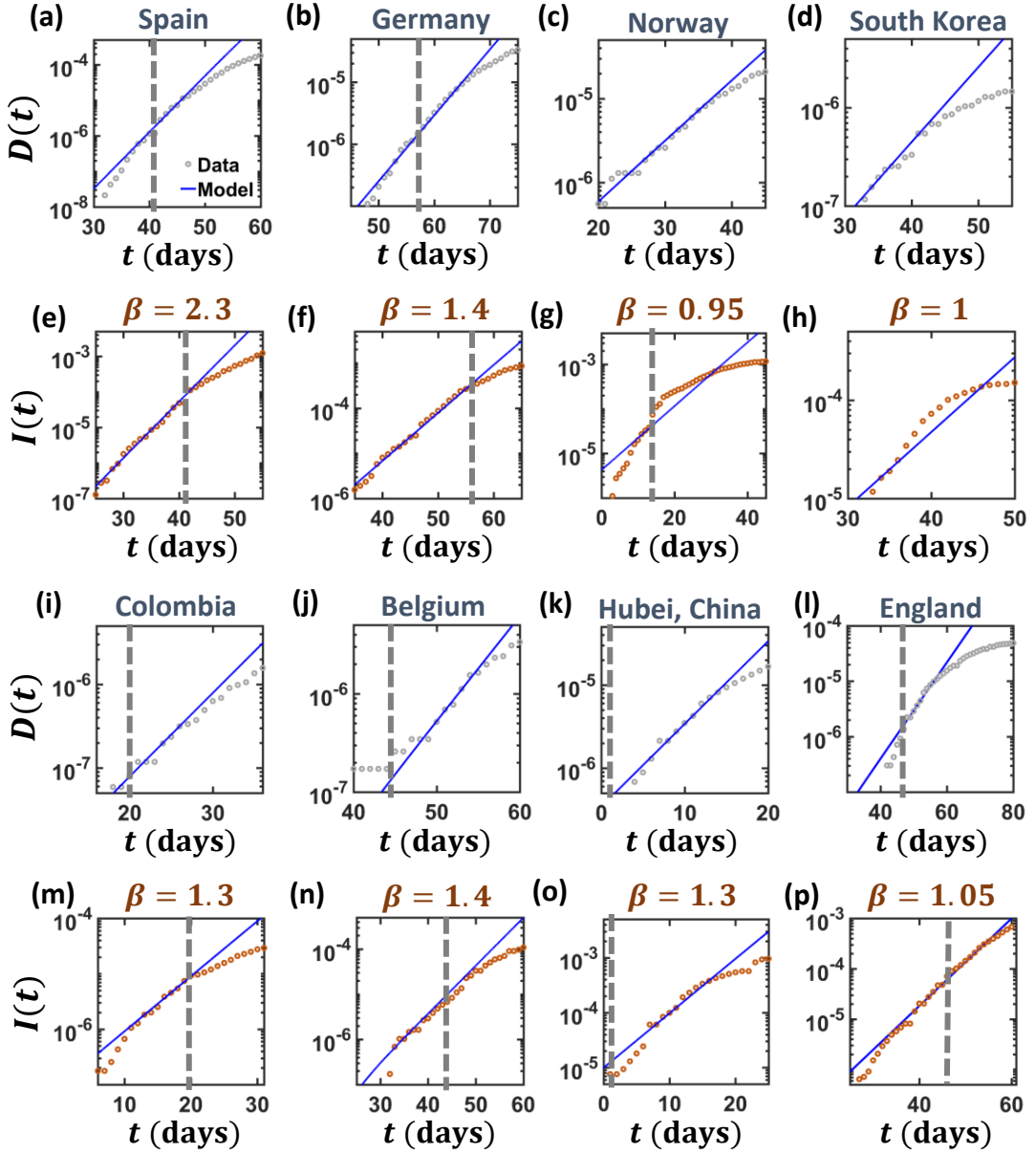


FIG. 8: Analysis of the empirical spreading dynamics. We tracked the mortality in 14 different countries, 8 shown here (grey circles), and 6 in Fig. 2 of the main text. Extracting the exponential slope (blue solid lines) we evaluated the infection rate  $\beta$ . This allowed us to predict  $I(t)$  in each country, and match with the empirical data (orange circles).

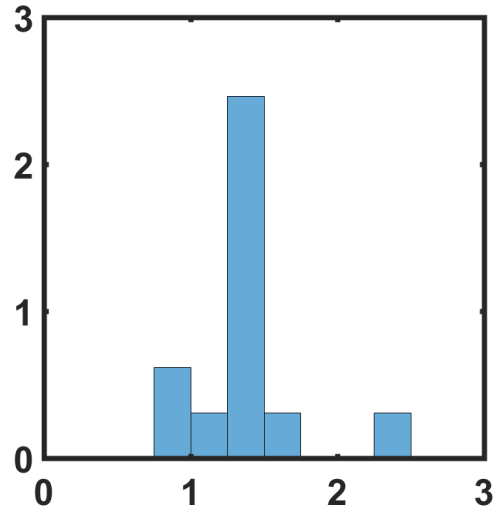


FIG. 9: **The variability of infection rates among countries.** Histogram of the estimator  $\hat{\beta}$  values by countries